Optimal Design of Nonlinear Periodic Electrical Networks for Soliton Pulse Generation

Andrew Gusty
University of Colorado Boulder
Computer Science and Applied Mathematics

Advising Committee
Dr. Elizabeth Bradley, Dr. Fruzsina Agocs,
Dr. Emily Jensen, and Dr. Cody Scarborough

Senior Thesis Proposal

Abstract

Nonlinear transmission lines (NLTLs) offer a reliable, low-cost platform for generating high-power RF pulses, but their design remains largely empirical or limited to small-amplitude approximations. This project develops a tractable analytical-computational framework to design nonlinear periodic electrical networks that support soliton pulses with prescribed spectral and temporal properties. Using perturbation methods and soliton theory, a reduced-order continuum ODE model is derived which captures the soliton solutions of the full electrical network. This model is used to formulate an ODE-constrained optimization problem that enables tuning of the network's dispersion. Expected outcomes include numerical solutions of the proposed optimization problem, verification of these solutions through simulations of the full discrete network, and a general framework that can be used to inform NLTL design.

1. Introduction

High-power radio frequency (RF) pulse generation is vital to technologies in defense, communications, and medical systems, including ultra-wideband (UWB), radar, and electronic countermeasure systems [1]. As these applications demand higher power, wider bandwidths, and improved energy efficiency, nonlinear transmission lines (NLTL) have emerged as promising platforms for synthesizing high-powered pulses from low-power input waveforms [2, 3, 4]. Compared to established vacuum and e-beam devices, NLTLs offer lower costs, accessible manufacturing, and can theoretically provide both high-power and high-frequency wideband operation [2, 5, 6], but their design and analysis require interdisciplinary expertise in electrical engineering, applied mathematics, and scientific computing.

NLTLs traditionally were used to modulate pulses mainly by decreasing the rise-time of an input square pulse [7, 8]. This modulation is made possible by the phase velocity, or speed of individual Fourier components propagating along a line, being directly related to their amplitude. On a NLTL with voltage-dependent capacitors or inductors, large-amplitude components move faster than low-ampltidue components, which can be exploited to sharpen an input pulse.

More recently, there has been great interest in the use of NLTLs for synthesizing high-power RF signals, following two important experimental studies. In the first, a NLTL with voltage-dependent ceramic capacitors

was used to produce 60 MW peak RF power at 100-200 MHz [4]. The second study used nonlinear inductors and linear capacitors in a NLTL-based modulator to produce 20 MW peak power at 1.0 GHz [3]. This device was the precursor to the current NLTL-based solid-state modulator sold by BAE systems, which produces over 25 MW peak power at 200 MHz - 2.0 GHz [9].

RF-pulse generation using NLTLs is accomplished by synthesizing a simple wave generated with a traditional e-beam device and inputting it to a NLTL. As the pulse propagates along the line, it evolves into a train or burst of sharp, stable pulses [2, 6, 10, 3], called *solitons* - special waveforms that propagate along a NLTL without distortion. The output burst has a significantly broader and higher spectrum than the input pulse, but only certain harmonics are enhanced strongly [2]. The effects of changing dispersion, line length, and type of nonlinearity have been experimentally investigated in [5, 6]. Some basic analytical expressions for the RF amplitude, the maximum voltage, and the central frequency of the generated pulses at each node of an NLTL have also been formulated using curve-fitting from experimental data in [10].

Using a NLTL-based solid-state modulator has several advantages over standalone e-beam devices [2, 9, 3]. Because NLTLs have no moving parts, they enjoy greater reliability and lower maintenance requirements than e-beam devices. In addition, transmission line components have a high degree of manufacturing maturity and wide availability of components, while also allowing for more compact and modular designs. However, a major barrier to deploying NLTLs in other high-power systems is the absence of a systematic framework for tuning an NLTL's parameters to synthesize solitons with prescribed amplitude, spectral content, and power. A general method for designing NLTLs would give insight into the limits of pulse modulation using solid-state devices, and would enable the expansion of NLTLs to applications in radar, medical imaging, and other RF domains beyond what has been achieved experimentally.

Optimizing the parameters of a NLTL is difficult because the equations governing the voltage dynamics of NLTL pulse propagation in discrete space are described by large systems of coupled nonlinear ODEs. In the case of an electrically long and weakly dispersive transmission line, the dynamics can be closely approximated by high-order nonlinear and dispersive wave equations on an infinite domain. For a long transmission line loaded by voltage-dependent capacitors, the dynamics of a small-amplitude pulse can be further reduced to the Korteweg-de Vries (KdV) equation [11, 2], which admits a family of stable, closed-form *solitary wave* solutions that give precise relations between the parameters of the NLTL and the soliton waveform it supports. In addition, the family of solitary wave solutions is asymptotically stable [12] with respect to a properly-weighted norm. One of the implications of this stability, is that a sufficiently smooth initial pulse will converge to one or more soliton solutions in a traveling reference frame for the KdV equation [11].

However, these remarkable analytical results are limited to small-amplitude pulses, and practical systems rely on large, fast pulses propagating through dispersive lines, where these standard approximations lose validity. Nevertheless, experiments at practical operating powers and frequency show promising stability results: an input pulse evolves into a train of stable soliton pulses [2, 3, 4]. In these higher power and frequency regimes, analytical solutions are not known. However, by explicitly computing stationary soliton profiles rather than simulating the full spatiotemporal pulse evolution, the supported waveforms of a given network can be obtained efficiently using the iterative numerical approach of [13], which fully captures the nonlinear and dispersive behavior of the circuit. The present work makes use of soliton theory to solve the inverse of the problem in [13]: rather than determining the soliton supported by a given network, we seek to design the network parameters themselves to support a prescribed soliton pulse.

The proposed outcome of this thesis is to solve an optimization problem which optimizes the dispersion of a NLTL using voltage-dependent capacitors, in order to synthesize a waveform with a desired spectral profile. We accomplish this by using perturbation methods to derive a reduced-order model of the voltage

dynamics which describes the solitary wave solutions supported by the line. This serves as a constraint in the optimization problem, which can be solved using numerical methods. The rest of this proposal is outlined as follows: in section 2, the periodic electrical network structure is presented as well as a reduced order model of the voltage dynamics which captures the solitary wave solutions of the full network. In section 3, an optimization problem is formulated based on this model and the goals and future directions of the thesis are discussed. Sections 4 and 5 address the intellectual merit and broader impacts of this thesis respectively. Involved derivations are included in appendices to streamline the presentation.

2. Work Completed

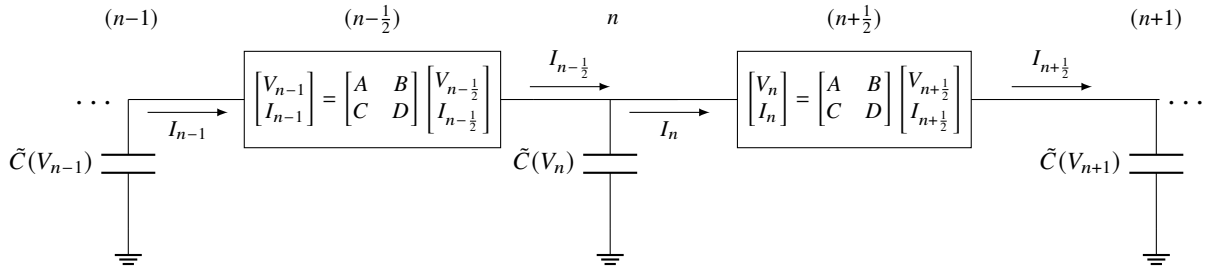

Figure 1: Circuit diagram of the nonlinear periodic electrical network with ABCD matrix representation for each linear component.

Consider the infinite one-dimensional periodic electrical network shown above. We model the network as unit cells of uniform length $\ell > 0$, indexed by integers $i \in \mathbb{Z}$. Each unit cell consistent of two linear components which can be described by their ABCD matrices, loaded by a voltage-dependent capacitance $\tilde{C}(V_i)$. We use ABCD matrices because they can be applied to any two-port linear component and provide algebraic relations between the current and voltage entering and exiting the component, which enables straightforward derivations. The length of each cell ℓ is defined as the distance between two capacitors, which form the boundary of each unit cell, with the linear two-port network governing the inner dynamics of the unit cell. The entire structure is assumed to extend infinitely in space.

Parameter	Definition	Units
L_0	TL Inductance per Unit Length	$\frac{V \cdot s}{A \cdot m}$
C_0	TL Capacitance per Unit Length	$\frac{A \cdot s}{V \cdot m}$
ℓ	Unit Cell Length	m
Z_0	Unit Cell Characteristic Impedence	Ω
β	TL Propagation Constant	$\frac{1}{m}$
$\tilde{C}(V)$	Voltage-Dependent Capacitance	$\frac{A \cdot s}{V}$

Table 1: Parameter value definitions and units for the considered NLTL model.

The time variable is denoted by $t \in [0, T] \subset \mathbb{R}$. The voltage at the i-th node is denoted $V_i(t) : [0, T] \to \mathbb{C}$, representing the electric potential difference at node i at time t. The current through the series element between nodes i and $i + \frac{1}{2}$ is denoted $I_i(t) : [0, T] \to \mathbb{C}$. It flows from node i to node $i + \frac{1}{2}$.

To enable an analytically tractable result, we consider the structure for the linear component below, which consists of only a transmission line:

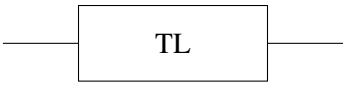

Kirchhoff's law, along with the definitions of the ABCD matrix, can be used to derive a system of discrete dynamical equations for the voltage of a pulse with a long wavelength relative to the electrical length of each unit cell:

$$(V_{n-1} - 2V_n + V_{n+1}) = \ell L_0 \frac{d^2}{dt^2}\left[V_n \cdot \tilde{C}(V_n) + \frac{\ell C_0}{2} V_n\right], \tag{1}$$

where the parameters are defined in Table 1. For a very long network where each linear component is a transmission line which is electrically small relative to the wavelength of pulse propagating along it, the discrete network behaves as a continuum [11]. We define $V(x,t)$ to be a smooth interpolating function of $V_n(t)$ such that $V_n(t) = V(n\ell, t)$ at every discrete spatial point $x_n = n\ell$. The dynamics can then be closely approximated by a spatially continuous PDE,

$$\left(\ell^2 \frac{\partial^2 V}{\partial x^2} + \frac{\ell^4}{12}\frac{\partial^4 V}{\partial x^4} + \frac{\ell^6}{360}\frac{\partial^6 V}{\partial x^6}\cdots\right) = \ell \bar{C} L_o \frac{\partial^2}{\partial t^2}\left[V(x,t)\left(\frac{\ell C_0}{\bar{C}} + F\big(V(x,t)\big)\right)\right], \tag{2}$$

where we have written $\tilde{C}(V) = \bar{C}F(V)$, where $F(V)$ is nondimensional and $\bar{C}$ has units of farads. Derivations of both (1) and (2) are provided in Appendix A. We note that the above PDE is the same as the PDE for the canonical infinite LC-ladder circuit with voltage-dependent capacitors described in chapter 3 of [11], up to different constants from the slightly different structures. If $F(V) := 1 - 2bv$ and the 6^{th}-order and higher dispersive terms on the left-hand side of (2) are ignored, then the result is the integrable 4th-order dispersive equation described in section 3.2 of [11]. Alternatively, a perturbation method can be used when the pulse amplitude is small and nonlinearity is weak to approximate the dynamics to leading order using the KdV equation. We refer the reader to [8] for a derivation. Given these choices which lead to different equations of motion, it is important to carefully choose a scaling that gives a tractable, reduced-order model, while also remaining valid when the amplitude of a pulse is no longer small.

To recover such a model, we nondimensionalize (2) using the characteristic scalings,

$$v(x,t) = \frac{V(x,t)}{V_c}, \quad \chi = \frac{x}{x_c}, \quad \tau = \frac{t}{t_c}, \tag{3}$$

which leads to a 6th-order PDE that is approximately valid for a pulse with amplitude of $O(\varepsilon)$ as $\varepsilon \to 1$. The dynamics are approximate because we truncate the 8th-order and higher derivative dispersive terms, with the assumption that the infinite series on the left-hand side of (2) converges. The dynamics can further be reduced to a 4th order ODE if we limit our solutions to solitons - i.e. a pulse with constant profile in the traveling coordinate $\xi = \chi - \bar{c}\tau$:

$$\frac{d^2 v}{d\xi^2} + \frac{2}{5}\delta^2 \frac{d^4 v}{d\xi^4} = \mu v - 2\pi_C v^2, \tag{4}$$

where parameter values can be found in Table 2, and a derivation of this reduced-order model can be found in Appendix B. This singularly perturbed, 4th-order differential equation describes the approximate profile of a soliton supported by the NLTL. Taking the critical limit as $\delta \to 0$ leads to an integrable hamiltonian system with the following solution (after converting back to a dimensional solution):

$$V(\xi) = \varepsilon V_0 \frac{3\mu}{4\pi_C}\,\mathrm{sech}^2\Big(\frac{\sqrt{\mu}}{2}\,k(x - ct)\Big), \tag{5}$$

Symbol	Definition	Description / Scale
x_c	$1/k$	Fundamental spatial harmonic of V_{target}
t_c	$1/\omega_0 = 1/(kc_{\text{lin}})$	Characteristic time scale corresponding to ω_0
c_{lin}	$\sqrt{\frac{1}{L_0C_0\left(1+\frac{\bar{C}}{\ell C_0}\right)}}$	Linear dispersionless wave speed
ε	$\frac{(k\ell)^2}{12} = \delta^2$	Small parameter quantifying dispersion strength
$\bar{c}$	c/c_{lin}	Nondimensional soliton speed
ξ	$\chi - \bar{c}\tau$	Traveling wave coordinate
V_c	εV_0	Voltage scale set by target soliton amplitude ($V_0 = O(1)$)
μ	$(\bar{c}^2 - 1)/\varepsilon$	$O(1)$ parameter representing deviation from c_{lin}
π_C	$2V_0\bar{c}^2\frac{b\bar{C}}{\ell C_0 + \bar{C}}$	Nonlinearity strength

Table 2: Summary of nondimensional variables and characteristic scales used to derive the reduced NLTL model.

a derivation of which can be found in Appendix C. This solution shows that pulse amplitude, width, and speed, are all dependent on the dispersion of the network captured by ε (or $\delta = \sqrt{\varepsilon}$). Thus, tuning the dispersion of the network gives control over all of these characteristics simultaneously.

3. Thesis Goals and Next Steps

Given a real, nondimensionalized target pulse to synthesize, V_{target}, we seek to tune the dispersion of the network shown in Fig. 1 to support a soliton pulse with similar spectral content to the target wave:

$$\min_{\delta\in[0,1]} \quad \|\tilde{V}(\xi) - V_{\text{target}}(\xi)\|_{L^2(\Omega)} \tag{6}$$

$$\text{subject to} \quad \frac{d^2v}{d\xi^2} + \frac{2}{5}\delta^2\frac{d^4v}{d\xi^4} = \mu v - 2\pi_C v^2, \quad v \in (-TT) \tag{7}$$

$$\text{on } \partial\Omega \quad \text{transparent and periodic boundary conditions} \tag{8}$$

$$\tilde{V}(\xi) = \text{Re}(v(\xi)), \tag{9}$$

We impose transparent and periodic boundary conditions to approximate an infinite spatial domain over a finite computational interval. Transparent boundaries minimize artificial reflections at the edges of the domain, ensuring that outgoing radiation does not re-enter the computational region, while periodicity allows for efficient representation of pulse trains or repeated structures. These conditions are implemented by linearizing the governing equation near the boundaries—where the pulse amplitude is small—and enforcing compatibility with the corresponding linear modes of the system. Together, they ensure numerical stability and physical accuracy without requiring an explicitly infinite domain.

Goal 1: Solve the constrained optimization problem in (6)–(9) numerically for different choices of V_{target}. To accomplish this, we will consider a periodic train of pulses centered on a closed, real interval $\Omega = [-T, T] \subset \mathbb{R}$, where $2T$ is the period of pulse repetition. The advantage of this reduced-order model is that it minimizes the size of the computational domain required for accurate solutions. Using Newton's method, the constraint equation (7) can be solved for small, nonzero $0 < \delta \ll 1$ using the soliton solution corresponding to $\delta = 0$ in (5) as an initial guess. Numerical continuation to slowly increase $\delta \to 1$ can then

be used alongside grid search or gradient descent to find the optimal value of δ.

Goal 2: Verify solutions from Goal 1 by simulating the full dynamics of the discrete network over a finite interval using a Finite-difference time-domain method (FDTD) with transparent boundary conditions. The simulation will be designed to simulate the network in a frame comoving at the same speed as the soliton. This means that only the edges of the pulse, which are small-amplitude, interact with the boundary, allowing for transparent boundary conditions based on the linearized dynamics in (29).

3.1 Ambitious Goals and Future Directions

Well-posedness: Formally establish the *existence and uniqueness* of solutions to the optimization problem defined in (6)–(9). This will require examining existence and uniqueness of solutions to the constraint in equation (7) on an infinite domain. This goal will draw on existing results for this type of system, which was studied in [14]. Proving well-posedness will provide a rigorous mathematical justification for the optimization framework and justify and specify the limits of using Newton's method with numerical continuation methods for $\delta > 0$.

Stability: Investigate the *stability properties* of the optimized soliton solutions obtained from Goal 1. By linearizing about the computed steady state and studying the spectrum of the resulting non-selfadjoint linear operator, we can identify whether the soliton solution is spectrally or asymptotically stable under small perturbations. This will connect the numerical optimization to analytical results in nonlinear wave stability theory.

Experimental validation: Construct nonlinear transmission line prototypes corresponding to different optimized parameter sets and target pulses to experimentally verify the predicted waveforms.

Generalization to other network structures: Extend the optimization and analysis framework to broader classes of periodic electrical networks, including those with nonlinear inductive elements and different linear components.

4. Intellectual Merit

Current designs of NLTL-based technologies for pulse synthesis rely on small-amplitude approximations and empirical tuning of discrete elements, limiting their ability to predict and control pulse spectra in strongly nonlinear, dispersive regimes. Soliton theory has historically provided analytical insight into NLTL behavior in weakly nonlinear limits [10, 11], but extending these results to higher amplitudes presents a major challenge because closed-form solutions to the governing dynamics are not known. This project develops a tractable optimization problem that uses soliton theory to connect the discrete circuit model to a reduced-order ODE retaining the dominant nonlinear and dispersive physics required for soliton propagation. This approach enables the systematic design of NLTL properties to synthesize desired pulses in a computationally efficient and physically interpretable manner, unifying circuit-level modeling with continuum descriptions of nonlinear wave propagation.

5. Broader Impacts

NLTL-based solid-state pulse modulators offer several advantages over conventional e-beam devices, including greater reliability, lower manufacturing cost, and improved modularity [2, 9, 3]. However, their use remains limited to a few domains, primarily ultra-wideband systems, because systematic design methods for tailoring NLTLs to specific radar, imaging, or directed-energy applications are not yet established. This

project addresses that limitation by developing a framework that enables precise tuning of NLTL dispersion and nonlinearity, extending the economic and operational benefits of NLTL technology to a wider range of high-power RF applications critical to national security and communications. The research also promotes involvement among applied mathematics, electrical engineering, and scientific computing, and presents opportunities for collaboration between academia and industry to develop NLTLs that are aimed at deployment in real systems. Finally, this project creates opportunities for undergraduates to develop numerical solvers and simulations, gaining early research experience in nonlinear dynamical systems, PDEs, and scientific.

References

[1] J. Benford, J. A. Swegle, and E. Schamiloglu, *High Power Microwaves*. CRC Press, 2016.

[2] J. D. C. Darling and P. W. Smith, "High-power pulsed RF extraction from nonlinear lumped element transmission lines," *IEEE Trans. Plasma Sci.*, 2008.

[3] B. Seddon, C. R. Spikings, and J. E. Dolan, "RF pulse formation in nonlinear transmission lines," in *IEEE Int. Pulsed Power Conf. (PPC)*, 2007.

[4] M. P. Brown and P. W. Smith, "High power, pulsed soliton generation at radio and microwave frequencies," in *IEEE Int. Pulsed Power Conf. (PPC)*, 1997.

[5] N. S. Kuek, A. C. Liew, E. Schamiloglu, and J. O. Rossi, "Circuit modeling of nonlinear lumped element transmission lines," in *IEEE Pulsed Power Conf. (PPC)*, 2011.

[6] N. S. Kuek, A. C. Liew, E. Schamiloglu, and J. O. Rossi, "Pulsed RF oscillations on a nonlinear capacitive transmission line," *IEEE Trans. Dielectr. Electr. Insul.*, 2013.

[7] E. Afshari and A. Hajimiri, "Nonlinear transmission lines for pulse shaping in silicon," *IEEE J. Solid-State Circuits*, 2005.

[8] M. M. Turner, G. Branch, and P. W. Smith, "Methods of theoretical analysis and computer modeling of the shaping of electrical pulses by nonlinear transmission lines and lumped-element delay lines," *IEEE Trans. Electron Devices*, 1991.

[9] C. R. Spikings, N. Seddon, R. A. Ibbotson, and J. E. Dolan, "HPM systems based on NLTL technologies," in *IET Conf. High Power RF Technol.*, 2009.

[10] M. Samizadeh Nikoo, S. M.-A. Hashemi, and F. Farzaneh, "Theory of RF pulse generation through nonlinear transmission lines," *IEEE Trans. Microw. Theory Techn.*, 2018.

[11] M. Remoissenet, *Waves Called Solitons: Concepts and Experiments*. Springer, 1999.

[12] R. L. Pego and M. I. Weinstein, "Asymptotic stability of solitary waves," *Commun. Math. Phys.*, 1994.

[13] J. Johnson and C. Scarborough, "Iterative technique for computing soliton solutions to periodic nonlinear electrical networks," *Opt. Mater. Express*, 2024.

[14] E. Lombardi, "Orbits homoclinic to exponentially small periodic orbits for a class of reversible systems. application to water waves," *Arch. Ration. Mech. Anal.*, 1997.

A. Derivation of the Voltage Dynamics

By continuity of the voltage, along with the definition of the ABCD matrix, we have

$$V_{n-\frac{1}{2}} = V_n = AV_{n+\frac{1}{2}} + BI_{n+\frac{1}{2}} \tag{10}$$

$$\implies I_{n+\frac{1}{2}} = \frac{1}{B}(V_n - AV_{n+\frac{1}{2}}) \tag{11}$$

$$I_n = CV_{n+\frac{1}{2}} + DI_{n+\frac{1}{2}} \tag{12}$$

substituting (11) into (12) yields,

$$I_n = CV_{n+\frac{1}{2}} + \frac{D}{B}(V_n - AV_{n+\frac{1}{2}}) \tag{13}$$

Following the same process yields the above equations for any $n \in \mathbb{Z}$, which gives the current at each point in terms of the voltage. Note that for our structure, it can be assumed that $B = i\omega\tilde{B} := \frac{d}{dt}\tilde{B}$ in the time domain

since the above equations describe a linear system, we can recover the dynamics from the algebraic ABCD relations. Using this fact, we can rewrite (11) and (13) as,

$$\dot{I}_{n+\frac{1}{2}} = \frac{1}{\tilde{B}}(V_n - AV_{n+\frac{1}{2}}) \tag{14}$$

$$\dot{I}_n = \frac{1}{\tilde{B}}(DV_n - (AD - BC)V_{n+\frac{1}{2}}) \tag{15}$$

$$\implies \dot{I}_n = \frac{1}{\tilde{B}}(AV_n - V_{n+\frac{1}{2}}), \tag{16}$$

where we use the fact that $A = D$ and $AD - BC = 1$ for the last step. We now analyze the charge drop over the capacitor at position n with voltage-dependent capacitance $\tilde{C}(V_n) = \bar{C}(1 - 2bV_n)$. Applying Kirchhoff's law yields,

$$I_{n-\frac{1}{2}} - I_n = \frac{d}{dt}\left[V_n \cdot \tilde{C}(V_n)\right] \tag{17}$$

$$\dot{I}_{n-\frac{1}{2}} - \dot{I}_n = \frac{d^2}{dt^2}\left[V_n \cdot \tilde{C}(V_n)\right] \tag{18}$$

$$\frac{1}{\tilde{B}}(V_{n-1} - AV_{n-\frac{1}{2}}) - \left(\frac{1}{\tilde{B}}(AV_n - V_{n+\frac{1}{2}})\right) = \frac{d^2}{dt^2}\left[V_n \cdot \tilde{C}(V_n)\right] \tag{19}$$

$$\frac{1}{\tilde{B}}(V_{n-1} - AV_n) - \frac{1}{\tilde{B}}(AV_n - V_{n+1}) = \frac{d^2}{dt^2}\left[V_n \cdot \tilde{C}(V_n)\right] \tag{20}$$

$$V_{n-1} - 2AV_n + V_{n+1} = \tilde{B}\frac{d^2}{dt^2}\left[V_n \cdot \tilde{C}(V_n)\right], \tag{21}$$

Where we have used the fact that our unit cell is symmetric and reciprocal, i.e. $A = D$ and $AD - BC = 1$. The next step is to compute the ABCD parameters of the unit cell, and plug them into the ODE, take a continuum limit, and arrive at a PDE.

Each unit cell consists of a transmission line, which has ABCD matrix:

$$\begin{bmatrix} V_{in} \\ I_{in} \end{bmatrix} = \begin{pmatrix} \cos(\beta\ell) & iZ_0 \sin(\beta\ell) \\ i\frac{1}{Z_0}\sin(\beta\ell) & \cos(\beta\ell) \end{pmatrix} \begin{bmatrix} V_{out} \\ I_{out} \end{bmatrix} \tag{22}$$

$$A = \cos(\beta\ell), \qquad B = iZ_0 \sin(\beta\ell) \tag{23}$$

Note that the ABCD matrices give algebraic relations in the frequency domain, such that ω corresponds to a temporal derivative in the time-domain. For $0 < \beta\ell \ll 1$, and using the fact that $\beta\ell = \omega\ell\sqrt{L_0C_0}$ for a transmission line, we can approximate A and B as,

$$A(\beta\ell) = 1 - \frac{(\beta\ell)^2}{2} + ..., \qquad 0 < \beta\ell \ll 1 \tag{24}$$

$$A(\beta\ell) \approx 1 + \frac{\ell^2 L_0 C_0}{2}\frac{d^2}{dt^2} \tag{25}$$

$$B(\beta\ell) = iZ_0\left(\beta\ell - \frac{(\beta\ell)^3}{6}\right) + O((\beta\ell)^5), \qquad 0 < \beta\ell \ll 1 \tag{26}$$

$$\approx i\omega\left(Z_0\sqrt{L_0C_0}\ell\right) \tag{27}$$

$$B(\beta\ell) = i\omega \underbrace{\ell L_0}_{\tilde{B}} \tag{28}$$

Where we have used the fact that $Z_0 = \sqrt{\frac{L_0}{C_0}}$. Substitution of the above into (21) yields (4).

B. Derivation of the Reduced-Order Model

To find appropriate scalings, we first linearize about a DC voltage $V_{bias} := 0$ w.l.o.g., $V(x,t) := 0 + \varepsilon\bar{V}(x,t)$, $0 < \varepsilon \ll 1$, then we have

$$\left(\ell^2\frac{\partial^2\bar{V}}{\partial x^2} + \frac{\ell^4}{12}\frac{\partial^4\bar{V}}{\partial x^4} + \frac{\ell^6}{360}\frac{\partial^6\bar{V}}{\partial x^6}\cdots\right) = \left(\ell^2 L_0 C_0 + \ell\bar{C}L_0\right)\frac{\partial^2}{\partial t^2}\left[\bar{V}(x,t)\right] \tag{29}$$

Let k be the wavenumber The dispersionless wavespeed is $c_{lin} = \sqrt{\frac{1}{L_0C_0\left(1+\frac{\bar{C}}{\ell C_0}\right)}}$. We then scale x by $x_c := \frac{1}{k}$, where k is wavenumber of the fundamental spatial harmonic of the desired waveform. Using this relation and the linear dispersionless wavespeed, we can scale t by the corresponding natural frequency corresponding to the wavenumber k for the dispersionless linearized equation, $t_c := \frac{1}{\omega_0} = \frac{1}{kc_{lin}}$. Note that we have in mind that $0 < (k\ell)^2 \ll 1$. The new PDE is,

$$(k\ell)^2\partial_\chi^2 V(\chi,\tau) + \frac{(k\ell)^4}{12}\partial_\chi^4 V(\chi,\tau) + \frac{(k\ell)^6}{360}\partial_\chi^6 V(\chi,\tau) + \cdots = (k\ell)^2\partial_\tau^2 V(\chi,\tau) - \frac{2b\bar{C}}{\ell C_0 + \bar{C}}(k\ell)^2\partial_{\tau\tau}\Big(V^2(\chi,\tau)\Big), \tag{30}$$

We set $\varepsilon := \frac{(k\ell)^2}{12}$. Before scaling V, we switch to a traveling coordinate $\xi = \chi - \bar{c}\tau$ to search for soliton solutions, where $\bar{c} = \frac{c}{c_{lin}}$ is the nondimensional wavespeed and c is the dimensional soliton wavespeed. Using this restriction reduces the above PDE to an ODE:

$$\frac{d^2V}{d\xi^2} + \varepsilon\frac{d^4V}{d\xi^4} + \frac{2}{5}\varepsilon^2\frac{d^6V}{d\xi^6} + \cdots = \bar{c}^2\frac{d^2}{d\xi^2}\Big(V(\xi) - \frac{2b\bar{C}}{\ell C_0 + \bar{C}}V^2(\xi)\Big). \tag{31}$$

Integrating twice and applying decay conditions at $\pm\infty$,

$$\varepsilon\frac{d^2V}{d\xi^2} + \frac{2}{5}\varepsilon^2\frac{d^4V}{d\xi^4} + \cdots = (\bar{c}^2 - 1)V - \bar{c}^2\frac{2b\bar{C}}{\ell C_0 + \bar{C}}V^2 \tag{32}$$

The goal is now to arrive at a scaling in which an analytically tractable solution is available. To accomplish this, we will start by imposing that $\bar{c}^2 - 1 = \varepsilon\mu$, where μ is an $O(1)$ constant (i.e. the dimensional soliton speed c is close to the dispersionless linear wavespeed c_{lin}). The resulting equation is a singularly perturbed 4th-order ordinary differential equation:

$$\varepsilon\frac{d^2V}{d\xi^2} + \frac{2}{5}\varepsilon^2\frac{d^4V}{d\xi^4} + \frac{1}{280}\varepsilon^3\frac{dV^6}{d\xi^6}\cdots = \varepsilon\mu V - \bar{c}^2\frac{2b\bar{C}}{\ell C_0 + \bar{C}}V^2 \tag{33}$$

Finally, we scale $\tilde{V} = \frac{V}{V_c}$ by the reference amplitude of the target wave, which we assume for now has maximum amplitude of $|V_{\text{target}}| \leq \varepsilon V_0$, where $V_0 = O(1)$, and $V_c = \varepsilon V_0$. Applying this and dividing both sides by ε^2 yields,

$$\frac{d^2\tilde{V}}{d\xi^2} + \frac{2}{5}\varepsilon\frac{d^4\tilde{V}}{d\xi^4} + \frac{1}{280}\varepsilon^2\frac{d\tilde{V}^6}{d\xi^6}\cdots = \mu\tilde{V} - 2\underbrace{V_0\bar{c}^2\frac{b\bar{C}}{\ell C_0 + \bar{C}}}_{:=\pi_C}\tilde{V}^2. \tag{34}$$

The solution to the above is the profile of a smooth interpolating function of the discrete system's voltage. Since the 6^{th}-order and higher derivatives are multiplied by small constants, independently of ε, we truncate the left-hand side side of (34) at 4th-order. This approximation will be validated by numerical simulations of the full system dynamics.

C. Derivation of the Solitary Wave Solution

We consider the reduced nonlinear ordinary differential equation in the critical limit as $\delta \to 0$

$$\frac{d^2v}{d\xi^2} = \mu v - 2\pi_C v^2, \tag{35}$$

where $\mu > 0$ and $\pi_C > 0$. We seek a bounded, symmetric solitary wave solution satisfying

$$v,\ v' \to 0 \quad \text{as} \quad |\xi| \to \infty,$$

where $()'$ denotes $\frac{d}{d\xi}()$. Multiplying (35) by $v'(\xi)$ and integrate once with respect to ξ:

$$\frac{1}{2}(v')^2 = \frac{\mu}{2}v^2 - \frac{2\pi_C}{3}v^3 + C.$$

Applying the boundary conditions $v, v' \to 0$ as $|\xi| \to \infty$ gives $C = 0$, so that

$$(v')^2 = \mu v^2 - \frac{4\pi_C}{3}v^3 = v^2\left(\mu - \frac{4\pi_C}{3}v\right). \tag{36}$$

Equation (36) is separable. For $v > 0$,

$$\frac{dv}{d\xi} = v\sqrt{\mu - \tfrac{4\pi_C}{3}v}. \tag{37}$$

Rearranging and integrating,

$$\int \frac{dv}{v\sqrt{\mu - \frac{4\pi_C}{3}v}} = \int d\xi. \tag{38}$$

Using a u-substitution, let

$$u = \sqrt{1 - \frac{4\pi_C}{3\mu}v} \quad \Longrightarrow \quad v = \frac{3\mu}{4\pi_C}(1-u^2), \qquad dv = -\frac{3\mu}{2\pi_C}u\,du. \tag{39}$$

Substituting into (38) gives

$$-\frac{2}{\sqrt{\mu}}\int \frac{du}{1-u^2} = \xi - \xi_0. \tag{40}$$

Integrating,

$$-\frac{2}{\sqrt{\mu}}\tanh^{-1}(u) = \xi - \xi_0. \tag{41}$$

Solving for u and then v yields

$$u = \tanh\left[\frac{\sqrt{\mu}}{2}(\xi - \xi_0)\right], \tag{42}$$

$$v_0(\xi) = \frac{3\mu}{4\pi_C}\operatorname{sech}^2\left[\frac{\sqrt{\mu}}{2}(\xi - \xi_0)\right]. \tag{43}$$

We take $\xi_0 = 0$ for a pulse centered in the traveling frame. The scaling relations in (3) can be used to recover the dimensional voltage in (5).